

Supporting Information

Comprehensive resistive switching behavior of hybrid polyvinyl alcohol and TiO₂ nanotube nanocomposites from combining experimental and density functional theory studies

Ngoc Kim Pham^{1,2,*}, Nam Hoang Vu^{1,2,*}, Viet Van Pham¹, Hanh Kieu Thi Ta^{1,2}, Thi Minh Cao³,

Nam Thoai⁴, Vinh Cao Tran⁵

¹ Faculty of Materials Science and Technology, University of Science, Vietnam National
University, Ho Chi Minh City, Vietnam

² Center for Innovative Materials and Architectures, Vietnam National University, Ho Chi Minh
City, Vietnam (INOMAR)

³ Ho Chi Minh City University of Technology (HUTECH)

⁴ High Performance Computing Lab, Ho Chi Minh City University of Technology, Vietnam
National University, Ho Chi Minh City, Vietnam

⁵ Lab of Advanced Materials, University of Science, Vietnam National University, Ho Chi Minh
City, Vietnam

Table S1. Calculated lattice parameters and band gaps of TiO₂ anatase, PVA monoclinic and isolated PVA monomer of this work together with the reference experimental data. The values in parentheses were calculated using the optB88-vdW functional.

Lattice parameters	TiO ₂ anatase		PVA monoclinic		PVA monomer
	This work	Expt ^a	This work	Expt ^b	
a (Å)	3.800 (3.819)	3.782	7.856 (7.563)	7.81	2.47 (2.57)
b (Å)	3.800 (3.819)	3.782	2.55 (2.569)	2.52	
c (Å)	9.727(9.710)	9.502	5.37 (5.1636)	5.51	
β (°)			92°88' (93°60')	91°42'	
Band gap					
E _g (eV)	2.58 (2.0)	3.2	5.32 (5.53)	5.02 (This work)	4.83 (4.80)

a [1]

b [2]

Table S2. Comparison of FTIR vibrations of PVA-TiO₂ nanocomposites by using theoretical calculations and experiments

	Calculations			Experiments		Assignments
	PVA bulk	Isolated PVA	PVA-TiO ₂	PVA bulk	PVA-TiO ₂	
Wavenumber (cm ⁻¹)	3287 (vs)	3301 (vs)	3683 (m) 3583 (s)	3363 (vs)	3378 (w)	OH stretching
	-	-	3073 (vs)	-	-	OH stretching
	2967 (w)	2996 (w)	2996 (w)	2939 (s)	2945 (w)	CH ₂ stretching
	2882 (w)	2880 (w)	-	2878 (w)	-	CH ₂ stretching
	-	-	-	1735 (s)	1739 (w)	C=O group stretching
	1473 (s)	1464 (s)	1565 (m) 1464 (m)	1450 (m)	1460 (w)	CH ₂ bending
	1226 (vw)	1224 (vw)	-	1257 (m)	1265 (w)	CH wagging
	1130 (w)	1133 (w)	-	1103 (s)	1109 (m)	CH ₂ bending
	563 (m)	594 (m)	-	609 (s)	715 (m)	OH bending

vs: very strong, s: strong, m: medium, w: weak, vw: very weak in intensity

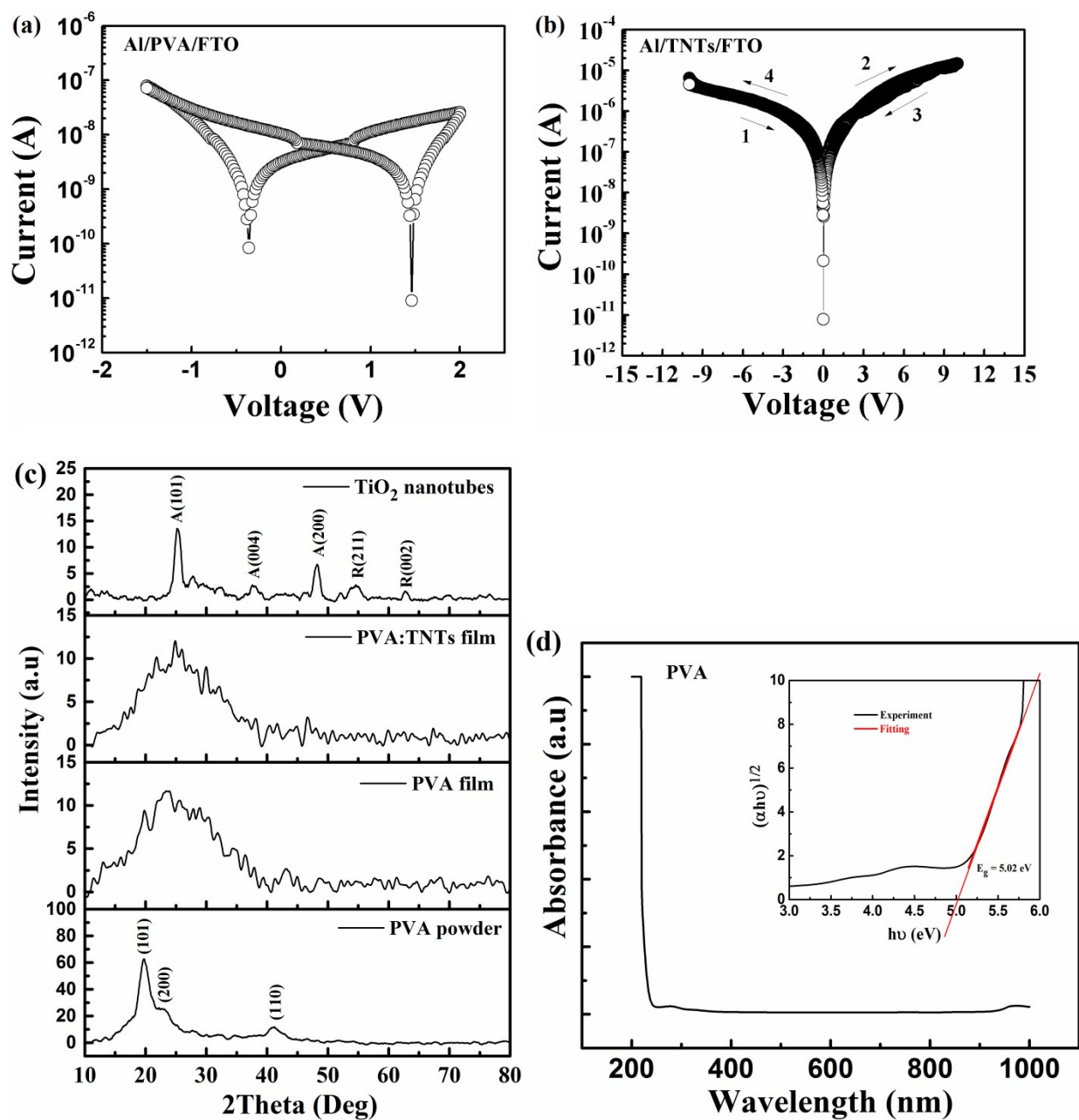


Figure S1. The current – voltage curve of Al/PVA/FTO (a) and Al/TNTs /FTO (b) device. XRD pattern of PVA, TNTs and nanocomposite thin films (c). Absorption spectra and band gap calculation from Tauc's plot of PVA inserted (d).

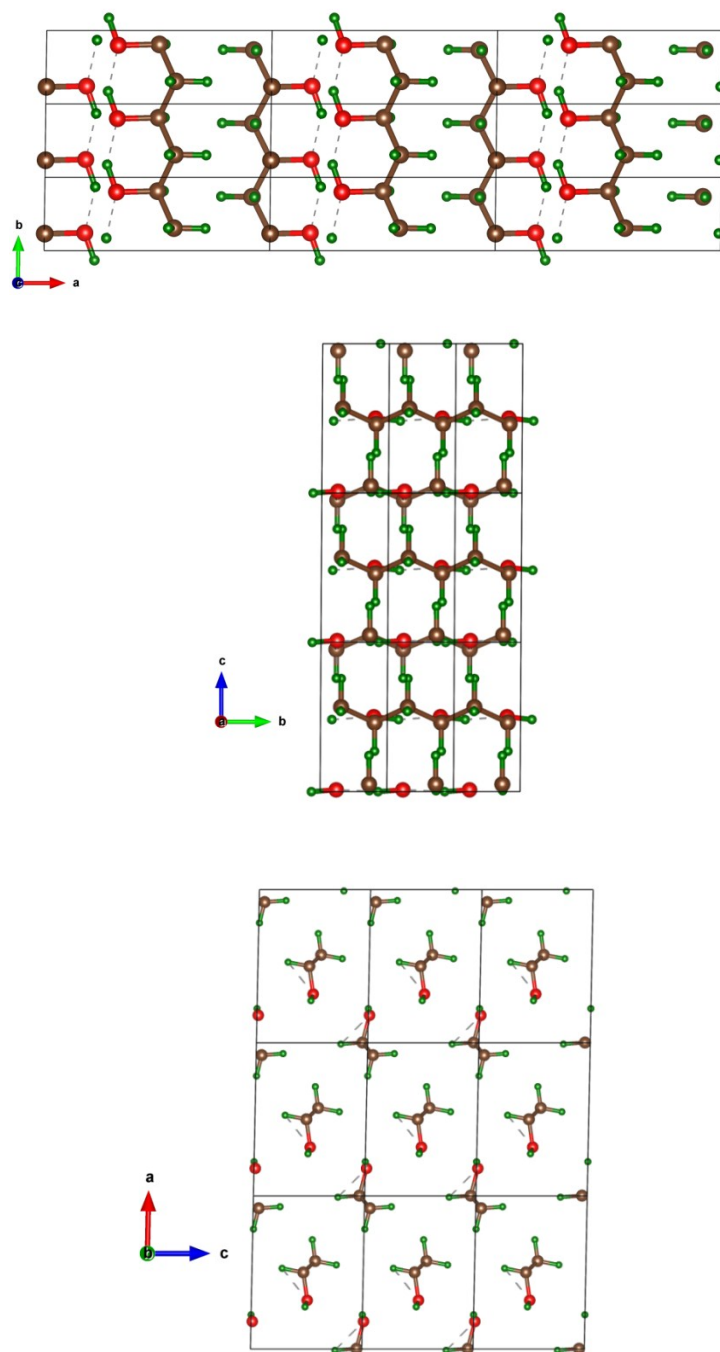


Figure S2. The atom structure of PVA monoclinic in (a) a, (b) b and (c) c direction of the lattice parameters. The one unit cell of PVA monoclinic is depicted by black lines.

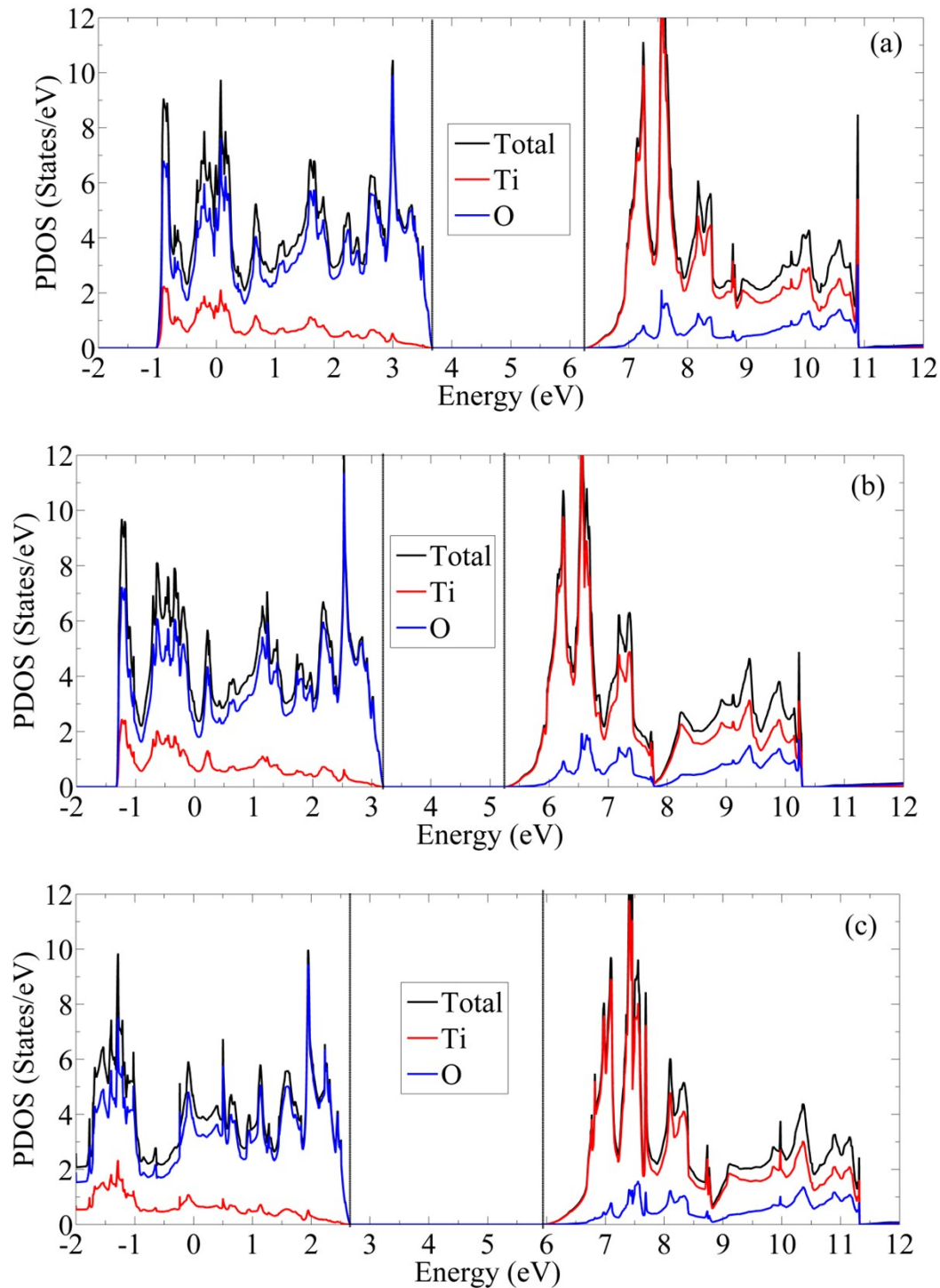


Figure S3. The partial DOS (PDOS) of TiO_2 anatase were calculated from the functionals of (a) PBE+U, (b) optB88-vdW and (c) HSE06. The VBM and CBM levels were indicated by the dashed line. The Fermi level is at the VBM level.

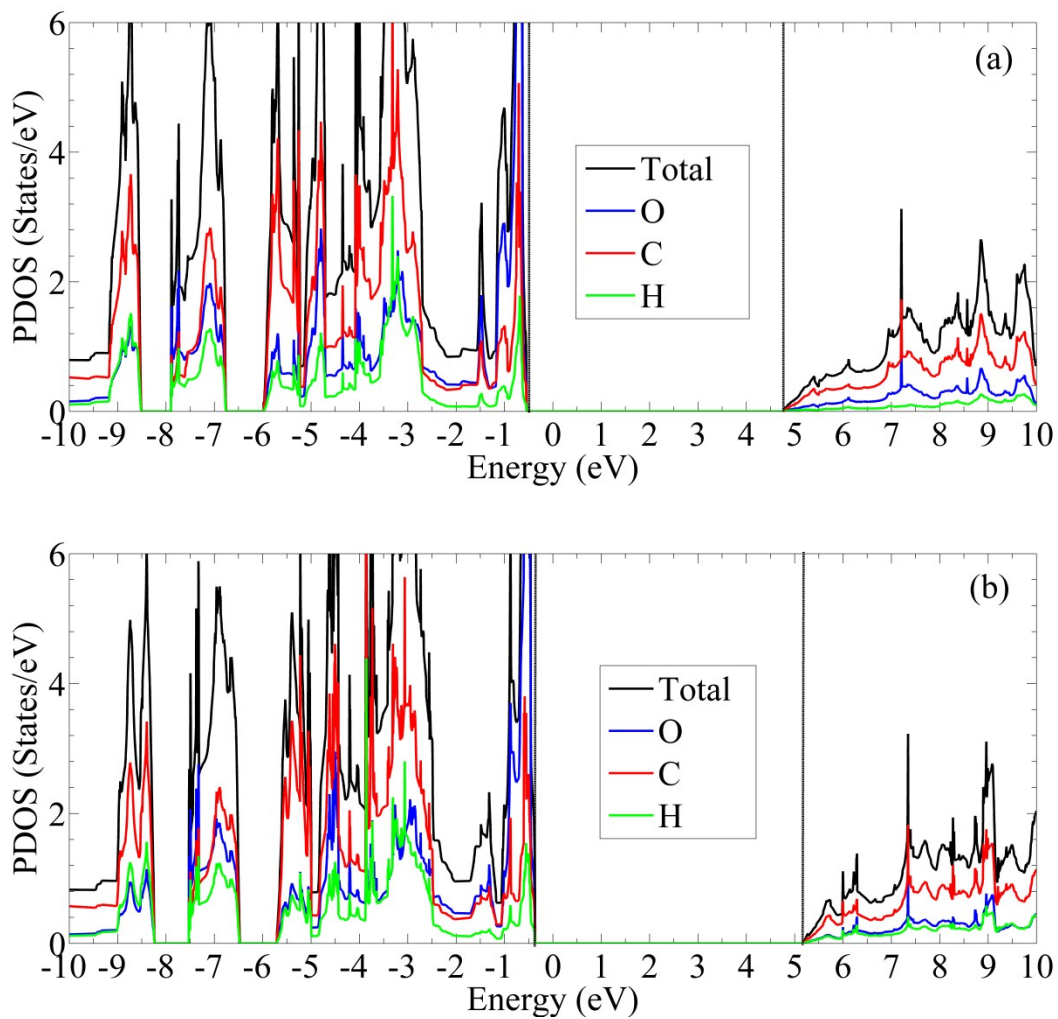


Figure S4. PDOS of PVA monoclinic in case of (a) the PBE functional and (b) optB88-vdW functional. The VBM and CBM levels were indicated by the dashed line. The Fermi level is at the VBM level.

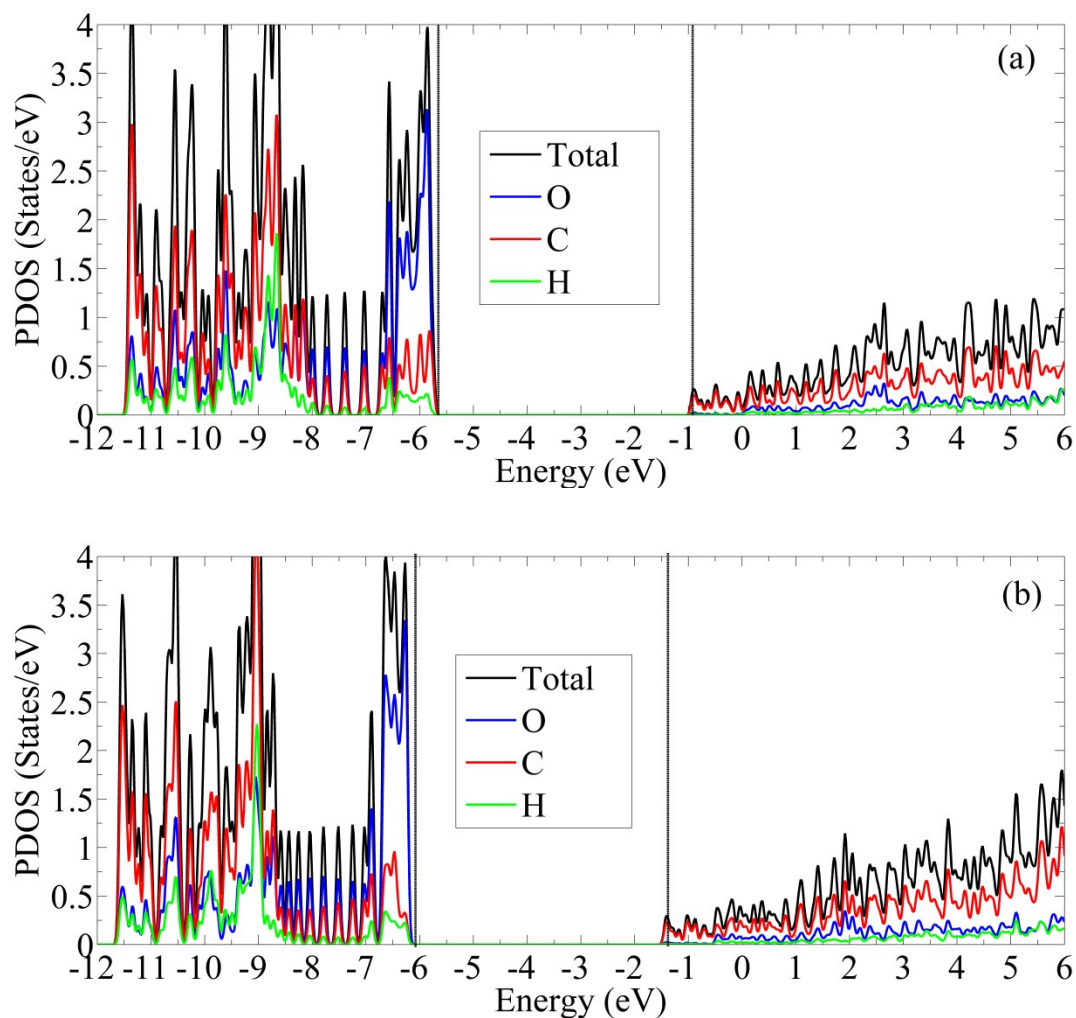


Figure S5. PDOS of isolated PVA monomer in case of the (a) PBE functional and (b) optB88-vdW functional. The HOMO and LUMO levels were indicated by the dashed line. The Fermi level is at the HOMO level.

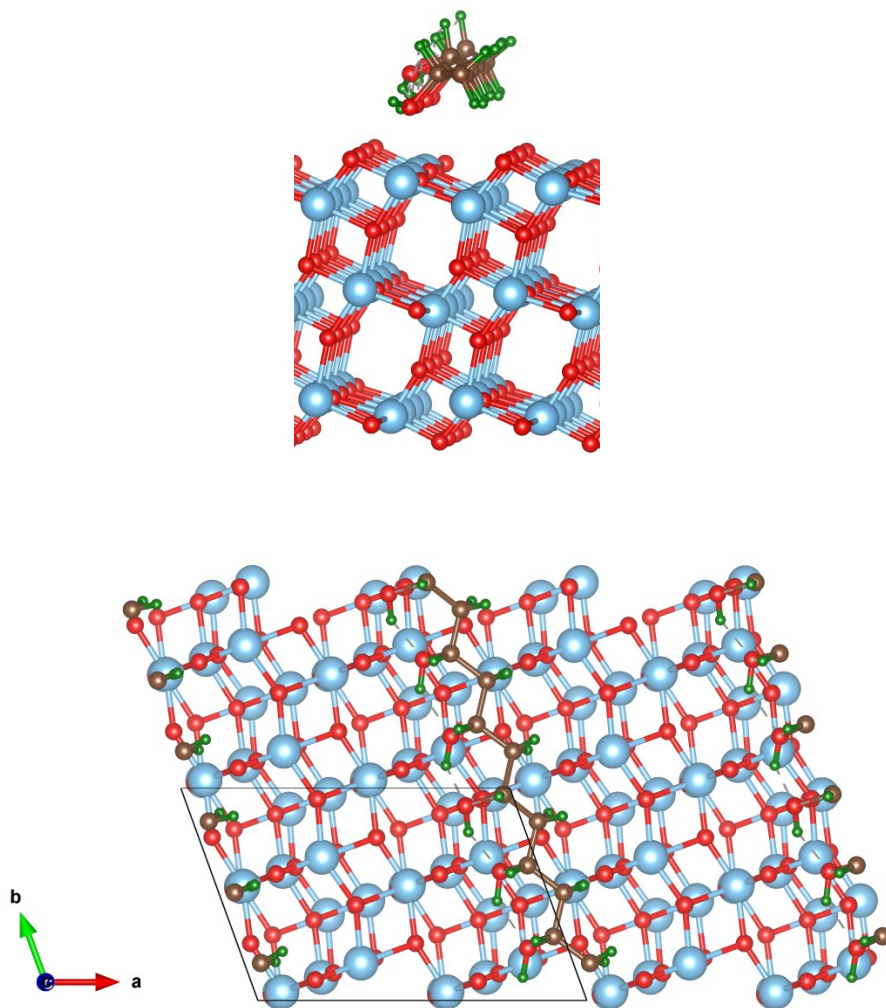


Figure S6. The atom model for the interface structure between anatase TiO₂(101) surface and PVA monomer with the binding energy of -0.69 eV. (a) side view and (b) top view. The 2×2 supercell of anatase TiO₂ (101) surface is depicted by black lines.

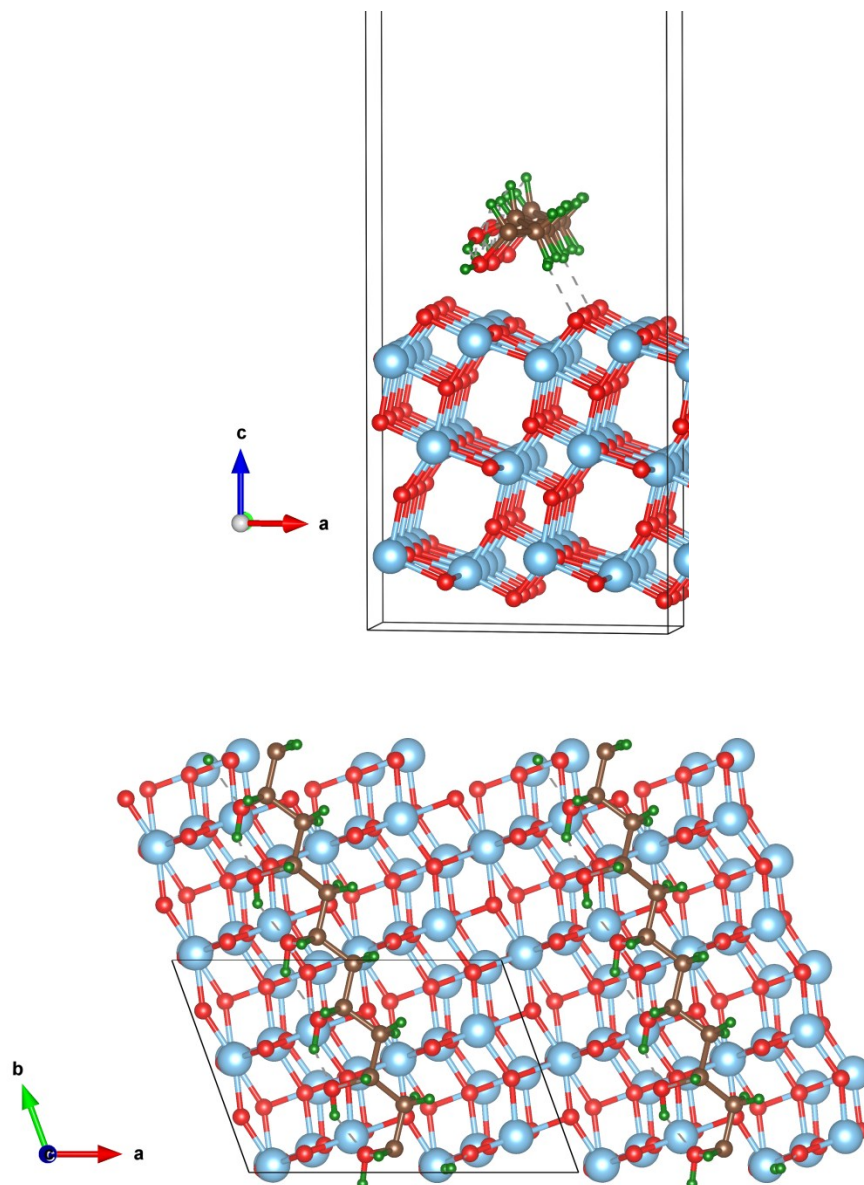


Figure S7. The atom model for the interface structure between anatase $\text{TiO}_2(101)$ surface and PVA monomer with the binding energy of -0.68 eV. (a) side view and (b) top view. The 2×2 supercell of anatase $\text{TiO}_2(101)$ surface is depicted by black lines.

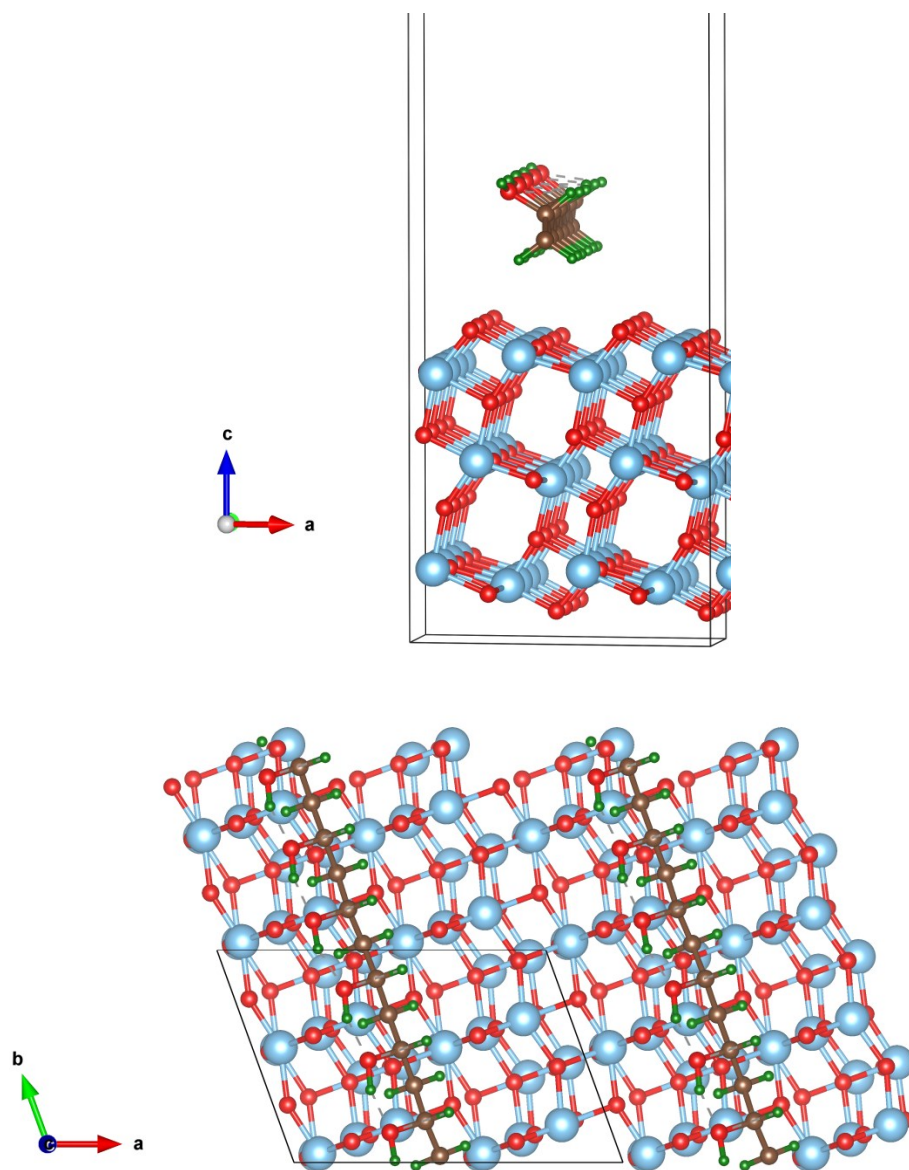


Figure S8. The atom model for the interface structure between anatase $\text{TiO}_2(101)$ surface and PVA monomer with the binding energy of -0.26 eV. (a) side view and (b) top view. The 2×2 supercell of anatase $\text{TiO}_2(101)$ surface is depicted by black lines.

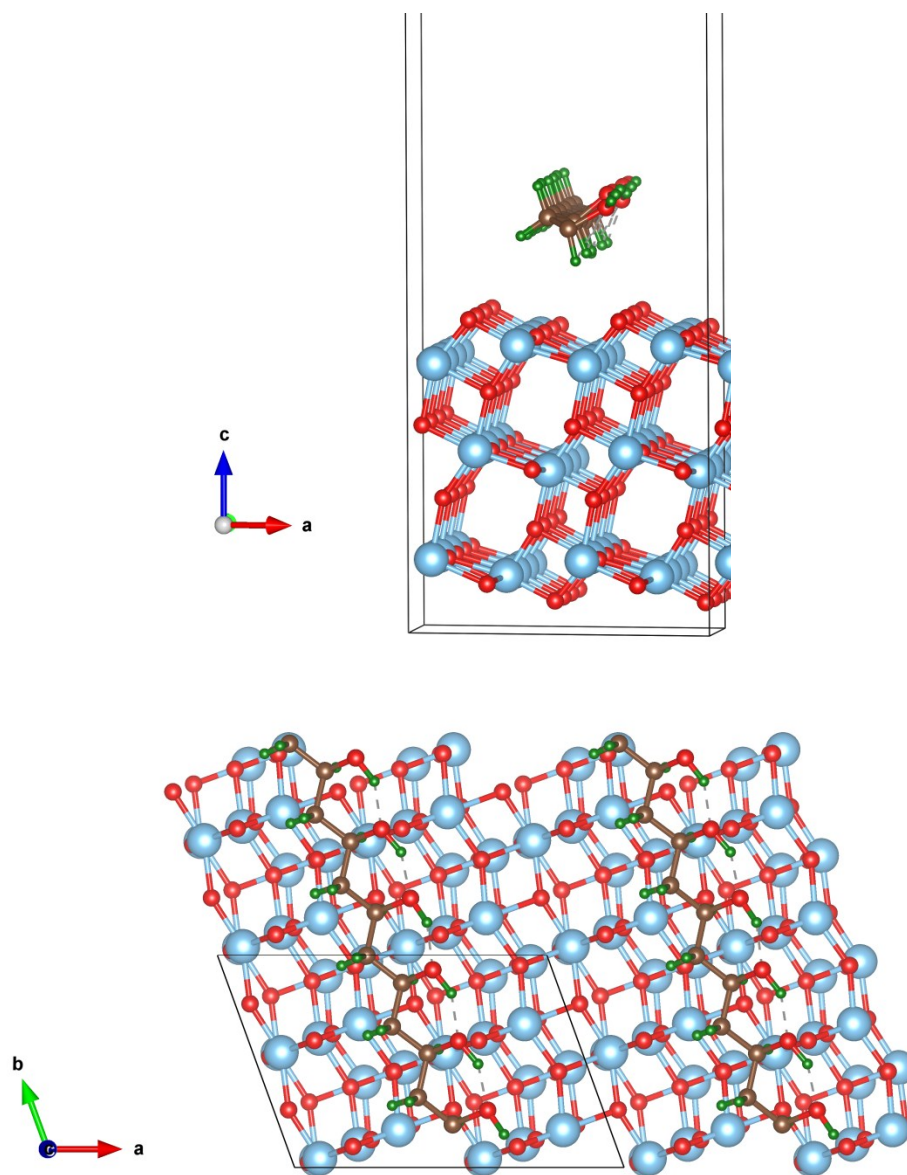


Figure S9. The atom model for the interface structure between anatase $\text{TiO}_2(101)$ surface and PVA monomer with the binding energy of -0.25 eV. (a) side view and (b) top view. The 2×2 supercell of anatase $\text{TiO}_2(101)$ surface is depicted by black lines.

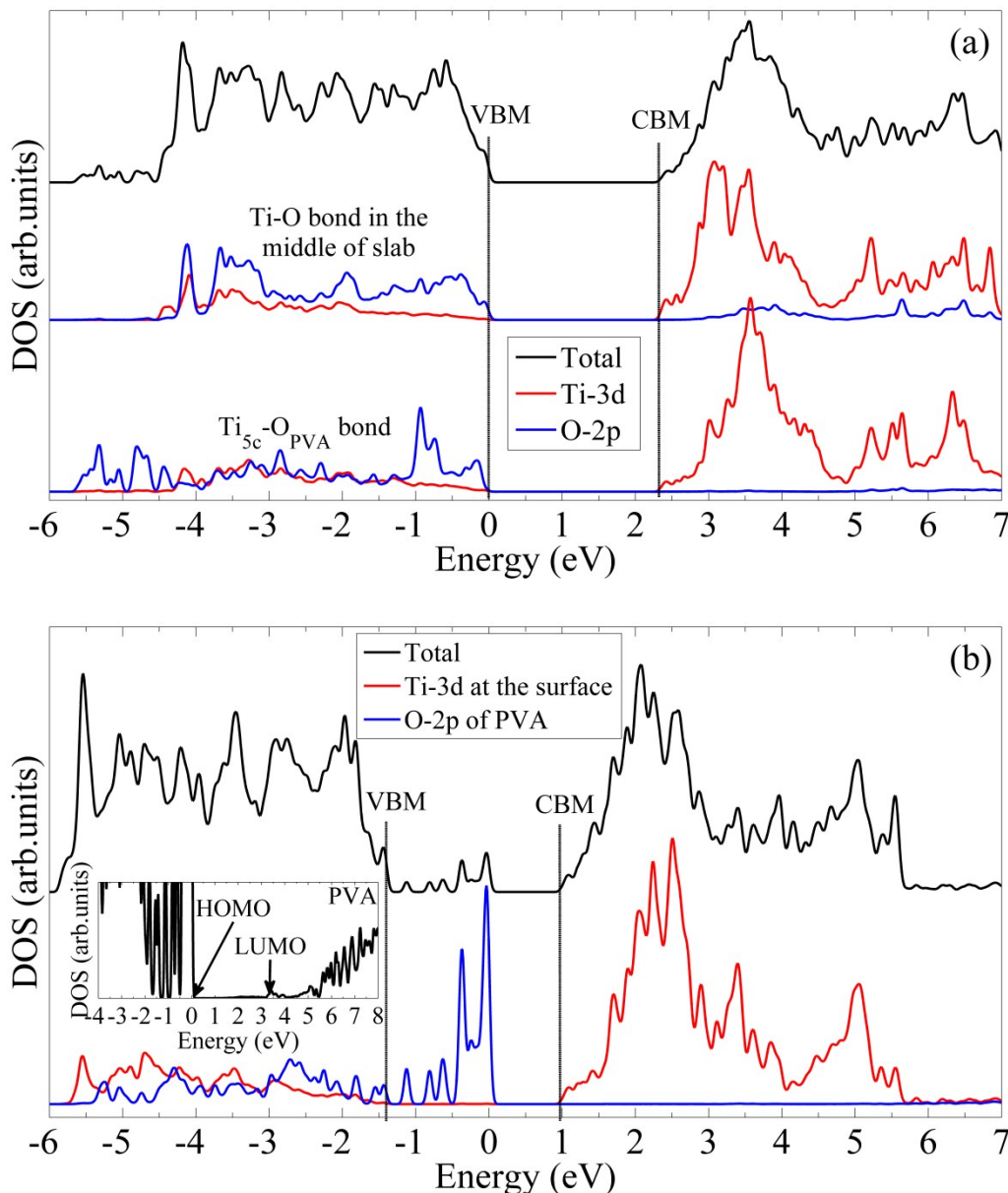


Figure S10. Project DOS on the d orbitals of the Ti atom (Ti-3d) and p orbitals of O atom (O-2p) calculated using the optB88-vdW functional for (a) the most stable structure in the middle of slab and at the interface region; and (b) the least stable structure at the interface region and the figure inset shows DOS of absorbed PVA with its HOMO and LUMO levels. The VBM and CBM levels were indicated by the dashed line. The Fermi level is at 0 eV.

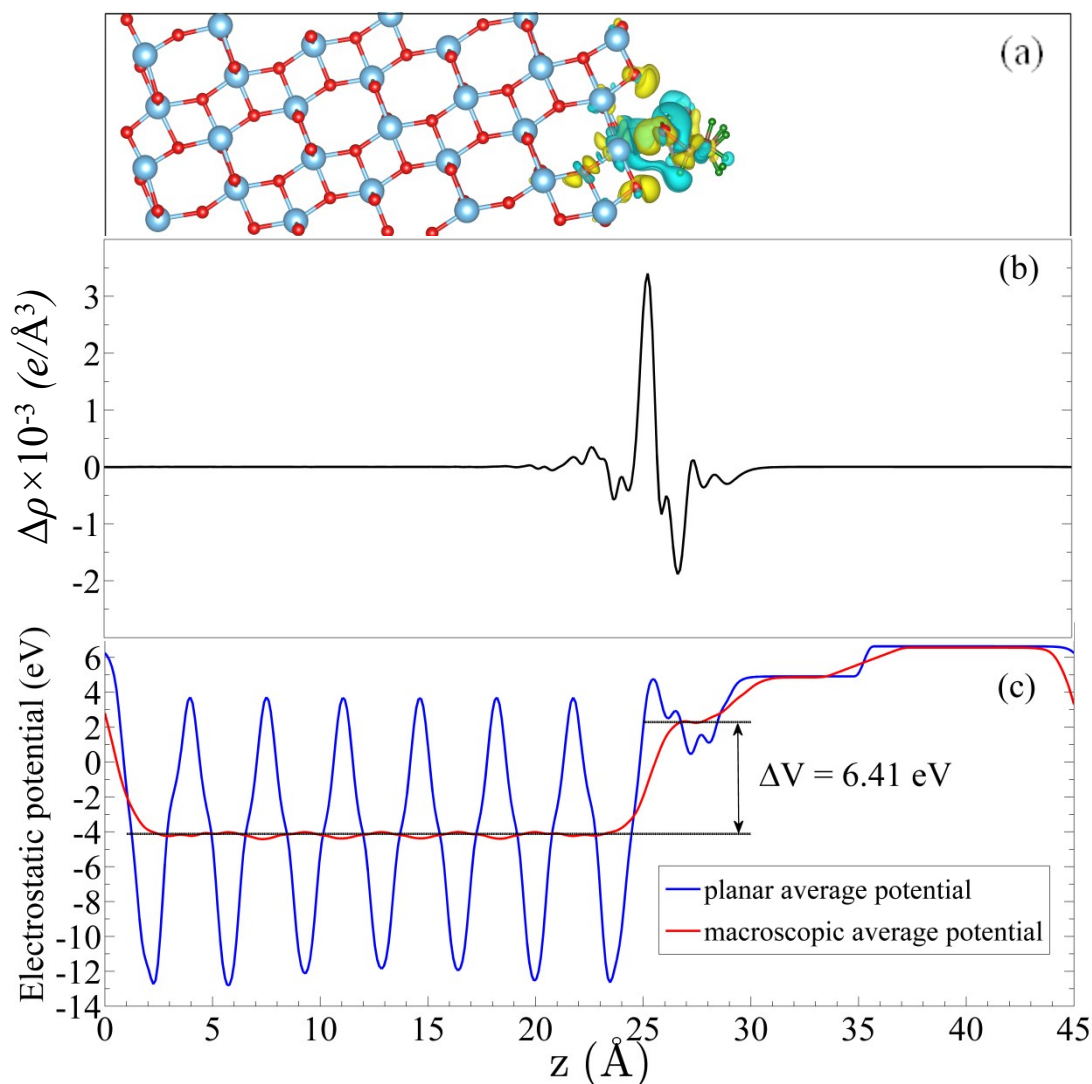


Figure S11. (a) The charge density difference of PVA on TiO₂(101) surface in an isosurface value of $\pm 0.001 e/\text{\AA}^3$ (+: yellow; -: cyan), (b) plane-averaged charge density difference in z-direction and (c) the planar average potential, macroscopic average potential and the built-in potential, $\Delta\bar{V}_{bi}$, of the most stable interface structure deriving from the optB88-vdW functional.

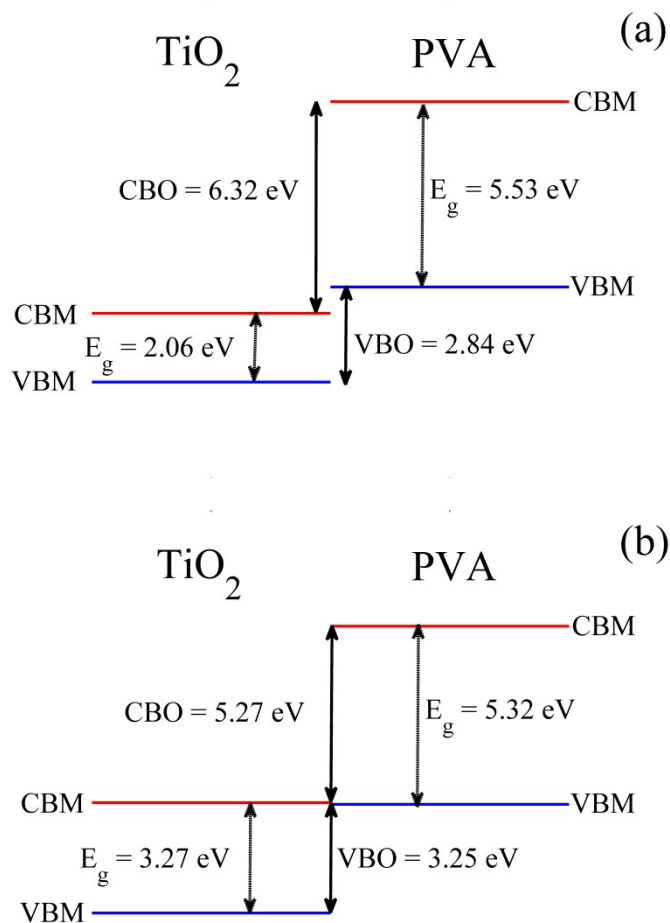


Figure S12. The schematic diagram of the band offsets of TiO_2/PVA composite deriving from (a) the optB88-vdW functional and (b) the mixed schema of the PBE+U and HSE06 functional.

References

1. Burdett, J.K., Hughbanks, T., Miller, G.J., Richardson, J.W. & Smith, J.V. Structural-electronic relationships in inorganic solids: powder neutron diffraction studies of the rutile and anatase polymorphs of titanium dioxide at 15 and 295 K. *Journal of the American Chemical Society* **109**, 3639-3646 (1987).
2. Colvin, B.G. Crystal structure of polyvinyl alcohol. *Nature* **248**, 756-759 (1974).